

A Reliable Framework for Human-in-the-Loop Anomaly Detection in Time Series

Ziquan Deng^{1,*}, Xiwei Xuan^{2,*}, Kwan-Liu Ma² (*Fellow, IEEE*), and Zhaodan Kong^{1,†} (*Senior Member, IEEE*)

Abstract—Time series anomaly detection is a critical machine learning task for numerous applications, such as finance, healthcare, and industrial systems. However, even high-performed models may exhibit potential issues such as biases, leading to unreliable outcomes and misplaced confidence. While model explanation techniques, particularly visual explanations, offer valuable insights to detect such issues by elucidating model attributions of their decision, many limitations still exist—They are primarily instance-based and not scalable across dataset, and they provide one-directional information from the model to the human side, lacking a mechanism for users to address detected issues. To fulfill these gaps, we introduce *HILAD*, a novel framework designed to foster a dynamic and bidirectional collaboration between humans and AI for enhancing anomaly detection models in time series. Through our visual interface, *HILAD* empowers domain experts to detect, interpret, and correct unexpected model behaviors at scale. Our evaluation with two time series datasets and user studies demonstrates the effectiveness of *HILAD* in fostering a deeper human understanding, immediate corrective actions, and the reliability enhancement of models.

Index Terms—Human-AI collaboration, time-series, anomaly detection, visual interface, XAI.

I. INTRODUCTION

Time series anomaly detection is a crucial technique in machine learning (ML), with broad applications such as identifying irregular financial transactions [1], monitoring abnormal health indicators in patient records [2], and preempting equipment failures in manufacturing [3]. Despite its importance, the effectiveness of these models can be compromised by biases—where models make decisions based on incorrect input features, resulting in problematic conclusions. To address this, eXplainable AI (XAI) techniques, especially visual explanations, are employed to shed light on models’ decision-making processes. However, these methods often focus on specific instances without scaling or generalizing insights across different data groups. Moreover, they solely allow a one-way information flow from models to users, without enabling users to verify and act upon the derived insights. To address these challenges, we introduce *HILAD*, a human-in-the-loop framework to enhance the robustness and reliability of anomaly detection models. Through a carefully-designed interface, our framework empowers experts to effectively detect,

interpret, and rectify model biases, thereby bolstering model performance and enhancing human trust. In the following, we delve deeper into different facets of our work.

A. Time Series Anomaly Detection Models

ML techniques for time series anomaly detection can be broadly categorized into unsupervised and supervised approaches. When ground-truth anomaly labels are unknown, unsupervised learning techniques are introduced to approximate future data points [4]–[6], where the deviations between the predicted and true values serve as anomaly indicators. On the other hand, if labeled data are available, supervised models can be trained as classifiers to directly predict anomaly labels [7]–[9]. Such models can often achieve higher accuracy and be utilized in critical areas like fraud detection or medical diagnostics [10], [11]. However, supervised models are generally more susceptible to bias issues, causing significant risks [12]. Considering this, in our work, we focus on enhancing supervised models with a CNN architecture, aiming to detect, understand, and mitigate hidden biases in such models with a human-in-loop approach.

B. XAI for Time Series Anomaly Detection

XAI methods are essential for enhancing transparency and building trust for time series anomaly detection models. Model agnostic approaches, such as LIME [13] and SHAP [14], attribute the model’s prediction of a specific instance to its features according to a surrogate model and game theory, respectively. Without the need to access models’ internal parameters, these methods are more generalizable for explaining various models, but fall short of specificity, tending to produce low-quality results, especially for deep models [15]–[17]. Contrastively, methods designed for specific model architectures can often provide more precise explanations with higher quality [18]–[20], despite compromising the flexibility to explain a broader range of models. For example, CAM and its variants [21], [22] are widely adopted in CNN explanations because of their capabilities of providing direct and intuitive explanations through heatmaps, highlighting which parts of the data mostly correspond to the model’s decision [23]. Specifically, CAM can assign a significance score to each time step of an input, indicating their temporal importance to a specific model prediction. Fig. 1 shows two time sequences with “anomaly” labels and a model makes “correct” predictions for both, where the actual periods that the anomaly happens are highlighted in blue and the model’s decision attributions provided by CAM are highlighted in green. In this example, it

¹Department of Mechanical and Aerospace Engineering, University of California, Davis, CA 95616, USA

²Department of Computer Science, University of California, Davis, CA 95616, USA

*These authors contributed equally.

†Corresponding author: Zhaodan Kong (e-mail: zdkong@ucdavis.edu).

This work was supported by NASA’s Space Technology Research Grants Program (grant number 80NSSC19K1052).

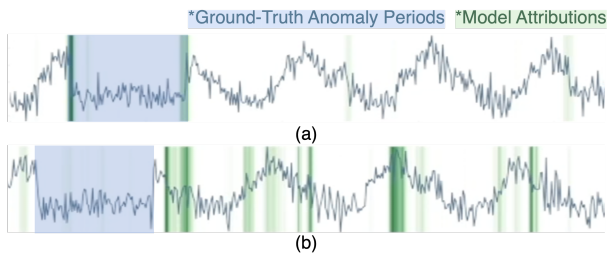


Fig. 1. Two sequences from the NASA MSL dataset with the ground truth label as “anomaly”. The true time frames corresponding to anomalies are highlighted in blue, and model’s attributes provided by CAM are highlighted in green. While the model makes “anomaly” prediction for both, regions highlighted by two colors overlap in (a) but not in (b), showing the model leverages the wrong features as the anomaly indicator in (b).

is clear that the blue and green regions overlap in (a) but not in (b), which means the model attributes anomaly prediction to normal time periods and generates seemingly correct results in (b). Example in (b) showcases the harmful model bias issue, and how CAM can detect such hidden issues.

C. Reliability Considerations of Models

Biased models can cause significant risks in real-world applications [24]. For instance, if a model identifies normal time series as anomalies, it underscores a fundamental misunderstanding of the underlying anomalous features, leading to potential overlooking of real anomalies [25]. While visual explanations such as CAM can reveal such discrepancies, their occurrence raises critical questions — Are these discrepancies a common feature across the entire data corpus, or are they isolated incidents? Moreover, once such biases are identified, what are the most effective methods for addressing and mitigating them? The discussion in Sec. I-B points out the limitations of current XAI techniques in fully tackling these challenges. This scenario necessitates further research and development of methods that not only highlight but also rectify these biases. Enhancing the reliability of anomaly detection models through improved understanding and correction of biases is essential to foster trust and ensure the efficacy of these systems in real-world applications.

D. Potential of Human-AI Collaboration

Handling model reliability issues in time series anomaly detection is fundamentally a human-centric task. The complexity of determining what constitutes an anomaly necessitates a deep understanding that goes beyond algorithmic detection, requiring expert judgment and contextual awareness that machines alone are not equipped to provide. Researchers have actively developed visual analytics (VA) systems that incorporate human knowledge into the loop, designing visualization techniques to assist in the analysis of complex datasets and models in time series anomaly detection. However, current methods mainly involve single-instance inspections and do not provide effective summarization of predominant issues, thus limiting their ability to enhance models at scale. Additionally, these methods often lack sufficient interpretability support and require extensive manual verification by experts. To overcome

these limitations, our work with *HILAD* aims to advance the state of the art by enhancing model interpretability, enabling the summarization and highlighting of critical data insights, thereby scaling up the integration of human knowledge into the machine learning process. *HILAD* is designed to streamline human-AI collaboration, making it more efficient at improving the accuracy and reliability of anomaly detection models.

E. Our Contribution

HILAD is a framework with an interactive interface, designed to enhance the reliability of ML models in the context of classification-based anomaly detection models. Our framework leverages visual explanation techniques to detect model biases, integrated with attribution-aware clustering and visual information summary to support group-level model issue interpretation and validation. The interface of *HILAD* navigates domain experts through the model validation workflow, facilitating the identification and mitigation of potential model biases. Simultaneously, *HILAD*’s spuriousness estimation mechanism allows humans to contribute domain knowledge at scale, where they manually annotate a few problematic clusters and then verify the estimated spuriousness of others. Lastly, we present a method for enhancing the model by rectifying identified errors based on human feedback. This bidirectional interaction supported by our framework utilizes human expertise effectively with a feedback loop, allowing humans to enhance AI systems with minimal effort.

To demonstrate the effectiveness of *HILAD*, we invite domain experts to conduct model enhancement studies with benchmark datasets, and design comparative analyses to systematically compare our approach with state-of-the-art baselines through quantitative performance evaluation. Our evaluation encompasses both objective metrics and subjective assessments and aims to investigate the following hypotheses:

- [H1] *Human-AI Collaborative Model Enhancement*. The performance of the *HILAD* framework, when aligned with human’s domain expertise at the decision level, is significantly superior to conventional automated algorithms that operate on a black-box machine learning model.
- [H2] *Human-Centric Model Interpretation*. Participants’ subjective insights, in terms of intuitiveness, transparency, and reliability, will be significantly enhanced by direct interaction with models through *HILAD* framework. In contrast, approaches that lack this synergy may face challenges in offering such perceptions.

Our contributions are summarized as follows:

- *HILAD*, a framework that integrates human expertise with ML techniques to enhance the reliability of time-series anomaly detection models, allowing for systematically detecting, interpreting, and mitigating model biases.
- An interactive VA interface allowing for model validation at different scales, supporting effective issue annotation and propagation with minimal but essential human efforts.
- A solution with humans in the loop for generating actionable insights and incorporating such insights in model enhancement, which can inspire future research on human-assisted trustworthy AI.

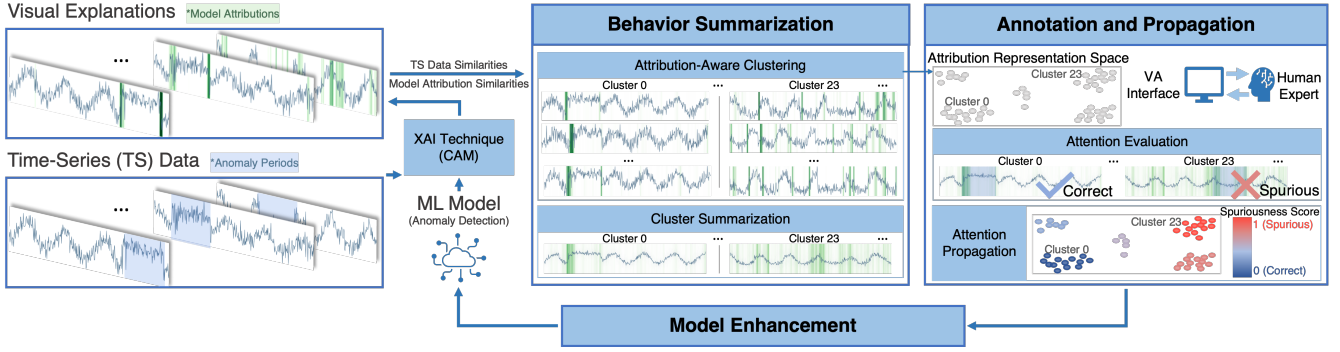


Fig. 2. The *HILAD* framework involves three main phases: “Behavior Summarization”, “Annotation and Propagation”, followed by “Model Enhancement”. With a time-series (TS) dataset and an anomaly detection model, we obtain model attributions with CAM. At the “Behavior Summarization” phase, we conduct attribution-aware clustering to obtain clusters with both similar TS data features and consistent model attributions, and we compute cluster summarization to aggregate each cluster’s pattern with a single visualization. At the “Annotation and Propagation” phase, users interact with our designed VA interface to identify and annotate model bias issues with the help of Spuriousness propagation. Lastly, the annotation and user-verified “Spuriousness score” are used at the “Model Enhancement” phase, which employs a model regularization method to mitigate detected model bias.

II. THE DESIGN OF *HILAD*

A. *HILAD* Framework

HILAD accepts a time-series (TS) dataset with ground-truth anomaly labels and a trained ML model for anomaly classification as input; provides an interactive interface for domain experts to detect and understand model issues; and supports issue mitigation with an integrated model regularization technique. Fig. 2 illustrates the framework of *HILAD*. In our quest for a model behavior interpretation that is intuitive and has the potential to be summarized, we employ an XAI technique, CAM [21]. With individual time sequences and an ML classifier for anomaly detection, CAM can produce visual explanations highlighting model attributions of its decisions. In our “Behavior Summarization” phase, we compute the similarity metrics of the original TS data and the model attributions, respectively, to conduct attribution-aware clustering from the latent space, as detailed in Sec. II-C. To enhance the efficiency of identifying model’s biased attribution issues, we further summarize each cluster with an integrated visualization, enabling experts to verify the attribution correctness without inspecting individual sequences. Our following “Annotation and Propagation” phase involves a visual interface for user interactions, where users overview clusters’ summarized model attributions, validate the exhibition of model issues, and annotate verified issues with a few clicks. As long as at least one cluster with “spurious attention” has been annotated, our backend method propagates the user’s assessment across other clusters as the estimated “Spuriousness scores”, enabling a facilitated model validation. Detailed explanations of this process can be found in Sec. II-D. After identifying the incorrect model’s attention, our model regularization strategy at the “Model Enhancement” stage systematically addresses these inaccuracies, refining the model’s focus to improve its overall performance and reliability, as described in Sec. II-E.

B. System Interface

The visual interface of *HILAD* comprises four main components. Fig. 3 depicts our interface when validating an anomaly classifier on the Mars Science Laboratory (MSL) dataset.

The System Menu (Fig. 3 A) provides options for configuration selections, including dataset, class, and visualization layout. Our primary objective is to analyze the model’s comprehension of anomalous patterns; therefore, we have configured the default class setting to represent anomaly-related instances, with ground-truth or prediction class as an anomaly. The Cluster Information (Fig. 3 B) presents an explainable behavior summarization for the current model in each cluster. Each cluster aggregates similar instances that garner analogous attention from the model. On the top of Cluster Information window, we introduce cluster metrics to facilitate navigation through the dataset. The available metrics, including Accuracy, Confidence, and Spuriousness — the latter derived via the Spuriousness Propagation method (Sec. II-E) contingent upon user annotation — are presented to enhance the rapidity of analysis. Once click/annotate one cluster in Cluster Information window, its corresponding position in 2D space will be highlighted in the Representation Space window (Fig. 3 C) and instances in this cluster will be detailed in the Instance Information window (Fig. 3 D). Two visualization layouts are available for Representation Space (Fig. 3 C): Scatter plot view or Detailed plot view, allowing for an overarching view of the similarity of clusters in 2D space or a more detailed inspection of each cluster. This function is also embedded in Representation Space to facilitate users to switch more flexibly. We also provide information on the correctness of the current model in terms of classification and attention.

Note that when interacting with the Representation Space window, the other two windows will be updated with coordinate information simultaneously to support user interpretation and issue verification. Due to the high similarity of adjacent clusters, when users annotate a cluster, they can quickly retrieve their neighbors in this window to speed up the annotation process. After a cluster is annotated in Cluster Information window, all instances of the cluster in Instance Information window have the same annotation by default. To further reduce the error introduced by the clustering algorithm, we allow users to adjust the annotations of individual data in the Instance Information window. The user must annotate data



Fig. 3. *HILAD* applied to the anomaly detection of a univariate time series classifier trained on the MSL dataset [26]. **A** System Menu, enabling the selection of dataset, class, and visualization options (Scatter plot view or Detailed plot view). **B** Cluster Information window, showing the data clusters and cluster metrics. **C** Representation Space window, showing a visual overview and the relative positions of all data clusters. **D** Instance Information window, showing individual time series sequences with model attributions belonging to a selected data cluster.

as correct or spurious at least once. Upon completing these annotations, the user can initiate model refinement by clicking the Retrain button. Subsequently, our backend algorithm will fine-tune the model in accordance with the user’s annotation, followed by an update to the model’s performance metrics shown in System Menu.

C. Behavior Summarization

At the “Behavior Summarization” phase, we first apply CAM to obtain model attributions correlated to its decision for each individual sequence. Then, we measure the similarities between: (1) the time-series data, according to the Dynamic Time Warping (DTW) Metric, and (2) the model attribution masks, according to the cosine similarity, respectively. With this information, we perform attribution-aware clustering to obtain clusters with similar data features and model attributions. To allow for effective user investigation, we visually summarize each cluster to help users identify common patterns of each cluster at a simple glance. We describe the details in the following.

1) *Time-series Context Similarity Calculation*: In the realm of time series analysis, assessing the similarity between sequences is a pivotal task. A prevalent technique to measure this similarity is the DTW algorithm, which strives to minimize the distance between two time-sequenced datasets by dynamically aligning and “warping” them in the time dimension. A smaller DTW distance indicates a higher similarity. Formally, for two multivariate time series $T_Q = \{T_{q_1}, T_{q_2}, \dots, T_{q_n}\}$ and $T_P = \{T_{p_1}, T_{p_2}, \dots, T_{p_m}\}$, $T_{q_i} \in \mathbb{R}^d$ and $T_{p_j} \in \mathbb{R}^d$, the DTW distance $d_{DTW}(T_Q, T_P)$ can be computed using the

following recursive formula:

$$d_{DTW}(T_Q, T_P) = d(T_{q_n}, T_{p_m}) + \min \begin{cases} DTW(T_{q_{n-1}}, T_{p_m}) \\ DTW(T_{q_n}, T_{p_{m-1}}) \\ DTW(T_{q_{n-1}}, T_{p_{m-1}}) \end{cases} \quad (1)$$

where $d(T_{q_n}, T_{p_m})$ is the Euclidean distance between vectors T_{q_n} and T_{p_m} . The initialization conditions are $D(T_{q_n}, T_{p_0}) = D(T_{q_0}, T_{p_m}) = \infty$ and $D(T_{q_0}, T_{p_0}) = 0$.

2) *Attribution Similarity Calculation*: Given a fully convolutional network (FCN), M , trained for time series binary classification task (i.e., normal or abnormal), an input time series sequence, T_Q , and the predicted class of the M for input T_Q , $c(T_Q)$, the attention score of T_Q is calculated as

$$a(T_Q) = CAM(M, T_Q, c(T_Q)), \quad (2)$$

where $a(T_Q)$ is a vector with the same dimension as T_Q , and each position in $a(T_Q)$ corresponds to the degree of dependence of model M on the corresponding dimension and time point when it makes the prediction $c(T_Q)$. Thus $a(T_Q)$ represents the model attribution. Please refer [21] to the specific calculation process of CAM. For input sequences T_Q and T_P , the attribution similarity, $d_{cos}(a(T_Q), a(T_P))$, is computed using the cosine distance as:

$$d_{cos}(a(T_Q), a(T_P)) = 1 - \frac{a(T_Q) \cdot a(T_P)}{\|a(T_Q)\|_2 \times \|a(T_P)\|_2}, \quad (3)$$

where $\|a(T_Q)\|_2$ and $\|a(T_P)\|_2$ denote the L2 norm of vectors $a(T_Q)$ and $a(T_P)$, respectively. Consistent with d_{DTW} , a smaller cosine distance indicates a higher similarity.

3) *Attribution-Aware Clustering and Summarization*: To aggregate data with similar context and also similar model

attribution together, we construct the following distance m_{QP} to measure the similarity between two instances T_Q and T_P :

$$m_{QP} = \alpha d_{DTW}(T_Q, T_P) + (1 - \alpha) d_{cos}(a(T_Q), a(T_P)), \quad (4)$$

where α is the weight to balance the data context similarity $d_{DTW}(T_Q, T_P)$ and the model attribution similarity $d_{cos}(a(T_Q), a(T_P))$. In this work, we set $\alpha = 0.5$ in all case studies. Thus, for all of the N time series instances, we can get the following distance matrix:

$$M_{dist} = \begin{bmatrix} m_{1,1} & m_{1,2} & \cdots & m_{1,N} \\ m_{2,1} & m_{2,2} & \cdots & m_{2,N} \\ \vdots & \vdots & \ddots & \vdots \\ m_{N,1} & m_{N,2} & \cdots & m_{N,N} \end{bmatrix}. \quad (5)$$

Finally, we use UMAP [27] to plot M_{dist} and apply K-means [28] to generate K clusters:

$$C = \text{K-means}(\text{UMAP}(M_{dist}), K), \quad (6)$$

where $C = \{c_1, c_2, \dots, c_K\}$ is the set of clusters, $\text{UMAP}(M_{dist})$ is the 2D representation of the data and K is the desired number of clusters. As a follow-up step, we visually summarize the resulting clusters as an integrated visualization for each cluster, which presents the common patterns of time sequences and model attributions in the current cluster, empowering users to grasp model behavior patterns more efficiently.

D. Annotation and Propagation

Building upon the aforementioned method, at the ‘‘Annotation and Propagation’’ phase, we To effectively evaluate such spurious attention, we introduce a metric termed ‘‘Spuriousness score’’, $S[c_i]$, ranging from 0 to 1, signifying the probability range from the least to the most likelihood of spurious attention occurrence. Furthermore, we deploy the Label Propagation [29], which automatically estimates probabilities of the unannotated clusters’ spuriousness based on users’ annotations and neighboring clusters $N(c_i)$ in the representation space.

The representation space is generated by UMAP as described in Sec. II-C, where we use the adjacency matrix, $A(i, j)$, to denote the distance between clusters’ feature representations of c_i and c_j . Notably, users only need to provide an annotation for one cluster (Algo. 1, Line 6), designating it as either ‘‘correct attention’’ ($S[c_i] = 0$) or ‘‘spurious attention’’ ($S[c_i] = 1$). Our algorithm (Algo. 1, Line 8-15) then propagates this information to compute Spuriousness scores for other clusters. Subsequently, these scores are showcased in the Cluster Information window (Fig. 3 B).

The ‘‘Spuriousness score’’ yields two noteworthy advantages. Primarily, they facilitate a more streamlined exploration process of clusters, with potentially spurious correlations being conspicuously highlighted. This is a pivotal step in aiding users to identify and assess problematic attention. Secondly, following users’ validation, these scores are leveraged to determine the problematic clusters crucial for issue mitigation, as we elucidate in the following section.

Algorithm 1 Label Propagation for Spuriousness Score

Require:

- 1: C : Set of clusters.
- 2: A : Adjacency matrix of clusters indicating similarity.

Ensure:

- 3: \mathbf{S} : Vector of spuriousness scores for each cluster.
 - 4: Initialize \mathbf{S} with -1 for all clusters.
 - 5: **for** each cluster c_i in C with a user label **do**
 - 6: $S[c_i] =$ label value of c_i
 - 7: **while** unlabeled clusters exist in C **do**
 - 8: **for** each unlabeled cluster c_i in C **do**
 - 9: $\text{WeightedSum}(c_i) = \sum_{c_j \in N(c_i)} A(c_i, c_j) \times S[c_j]$
 - 10: $\text{TotalWeight}(c_i) = \sum_{c_j \in N(c_i)} A(c_i, c_j)$
 - 11: $S[c_i] = \frac{\text{WeightedSum}(c_i)}{\text{TotalWeight}(c_i)}$
 - 12: **return** \mathbf{S}
-

E. Model Enhancement

An effective strategy for addressing detected spurious correlations in machine learning (ML) models involves model retraining or finetuning, which reduces the model’s resilience over potential bias while keeping the architecture intact. Retraining the model on a noise-corrupted dataset has demonstrated its efficacy in diminishing the model’s reliance on spurious features [30]. To counteract the influence of spurious features, we harness the masking strategy to shift and correct the model’s attention. The idea is conceptually simple: first, mask the parts of the data that receive spurious attention, then encourage the model to infer how to make decisions with the rest of the data. This idea has been used as a self-supervised pre-training method and spuriousness feature elimination method in Computer Vision (CV) and Natural Language Processing (NLP) fields. In our work, we adjust the Core Risk Minimization (CoRM) methodology [30] in the CV domain into time series data to introduce controlled masks into the annotated spurious attention time points by injecting random Gaussian noise into the data. This is also a fundamental data augmentation strategy called jittering for time series data that can help the model become more robust to variations and be used in masked autoencoder for time series forecasting task [31].

The integration of CoRM into *HILAD* entails several steps. First, after users annotate the data, we extract a set of instances, T_S , that display heightened probabilities of spuriousness, indicating undesirable attention. We also extract a set of instances, T_C , that display heightened probabilities of correctness, indicating correct attention. For the instances in T_S , pixel attributions (specifically, CAM masks) accentuate the spurious regions. We employ these masks to introduce random Gaussian noise to the identified spurious regions. Mathematically, for an individual time sequence $T_i \in T_S$, this operation can be succinctly represented as

$$T'_i = T_i + \mathbf{m} \odot z, \quad (7)$$

wherein T_i is the input time series data, \mathbf{m} denotes the CAM mask, z represents the generated Gaussian noise matrix, and \odot denotes the Hadamard product. Each variable is of the same

dimensions as the input time series data. Similarly, for $T_j \in T_C$, we add random Gaussian noise to the non-highlighted areas to enhance the model’s attention to abnormal patterns:

$$T'_j = T_j + (1 - \mathbf{m}) \odot z. \quad (8)$$

After substituting the original data with these spuriousness-masked and correctness-enhanced data, we proceed to re-train the model. Subsequently, an evaluation is conducted to determine the extent to which spurious correlations have been alleviated. In Sec. III-D, we elaborate on the evaluation metrics utilized to quantify the effectiveness of our method in mitigating spurious correlations.

III. EXPERIMENTAL DESIGN

In this section, we provide an experimental design to benchmark and evaluate the capabilities of *HILAD*. The primary objective of this experiment is to investigate how *HILAD* empowers humans to detect, understand, and correct potential issues in an anomaly classifier for time series data.

A. Task

In the experiment, participants were asked to interact with the interface of *HILAD* to evaluate a classification model trained on a specific dataset, containing both normal and abnormal time sequences. Specifically, we encouraged them to use as many visual components as possible, follow the system guidance to verify the highlighted issues, interpret them with the provided information, and annotate the confirmed errors in a restricted time. In each experiment, participants were only allowed to perform a single model retraining to better control experiment time and quantify the evaluation results.

With the awareness of the *HILAD* workflow, participants explored the general model behavior concerning different clusters of data through the Cluster Information window, where they also investigated further details from the Instance Information window that updated simultaneously with their interactions. They were asked to mark and annotate detection issues, such as a model using normal time points to determine an abnormal time series, which could be achieved by simply clicking the “Spurious” button in the Cluster Information window. At this point, all instances corresponding to this cluster were marked as spurious. Participants could further adjust the spuriousness labels of single instances in the Instance Information window. Similarly procedure could be conducted to label and adjust a cluster related to correct attention. As long as one cluster is annotated as spurious or correct, our algorithm will approximate the attention correctness of other clusters according to their similarities in the representation space, resulting in a spuriousness approximation score for every cluster. Participants can click the “spuriousness” button provided in our interface to rank clusters according to this score, allowing for adjustments and confirmation of the approximated model issues. When the participants confirmed the first round of issue inspection could be concluded, they would click the retrain button, and our system performed the model retraining based on the participants’ feedback.

B. Procedure

In the following, we introduce the experiment’s procedure. The overall practical accomplishment of the experiment took between 30 and 45 minutes.

1) *Introduction and Preparations*: Before the experiment begins, participants receive detailed instructions explaining the experiment’s purpose and overall structure before it begins. Next, they are introduced to the key concepts involved in time-series classification tasks, including metrics such as confidence and accuracy, possible abnormal patterns, and spurious model attention. Subsequently, an in-depth orientation to *HILAD* is provided, highlighting its various components and functionalities. This orientation covers the System Menu, Representation Space, Cluster Information, and Instance Information, elucidating their respective roles in detecting anomalies. The primary goal communicated to the participants is to employ *HILAD* for monitoring effectively and analyzing the model’s behavior, focusing on its attention mechanisms.

2) *Familiarization Procedure*: A simplified dataset was introduced to acquaint participants with the functions of the *HILAD* interface. This served as a practical tutorial on the tools available in each window. During this phase, participants gained insights into the relationships between different clusters and developed skills in identifying and annotating abnormal patterns. It is important to note that this segment was designed solely for hands-on learning, and its results were not included in the primary evaluation. Once participants demonstrated proficiency in accurately identifying and annotating abnormal patterns, they conducted the experimental run.

3) *Experimental Run*: In the experimental run, participants were introduced to the *HILAD* with two space domain-related datasets that mimic its real-world use for anomaly detection. Their task was to critically analyze the behavior of the classification model across the datasets. The main variable in this phase was the dataset itself, and the sequence of dataset presentation varied systematically among participants. This approach aimed to mitigate any potential bias from learning curve effects. We executed three trials for each dataset to further effectively compare the distinctions between the automated algorithm and the human-AI collaboration method. These trials varied in the scope of information provided to the participants: the first trial provided access to only the System Menu window, the second trial included System Menu, Cluster Information, and Representation Space windows, and the third trial offered a comprehensive view with the complete all of the four windows. The first trial in our study exemplifies the application of the automated algorithm, while the latter two trials represent the human-AI collaboration methods. To ensure the integrity of our results and eliminate any potential biases associated with the sequence of exposure, the order of these trials was randomized for each participant. This approach was essential to assess the impact of varying levels of information availability on the performance and decision-making processes in the context of human-AI interaction.

4) *Postprocessing*: Once all experimental runs are concluded, participants can reflect on the experiment and share their insights and feedback regarding *HILAD*. This qualitative data is gathered through questionnaires designed to assess

participants' subjective perceptions of human-AI cooperation, specifically focusing on intuition, transparency, and reliability. This data provides valuable insights into the user experience and the system's effectiveness in facilitating anomaly detection, evaluation, and correction.

C. Participants

This experiment was approved by the Institutional Review Board at the University of California, Davis. We involve 15 participants in total, of which 13 were male and 2 were female. All participants are graduate students between the ages of 23 to 30 years old. All participants passed the test to ensure they could accurately identify and annotate the abnormal pattern. All completed the entire experiment on two provided datasets.

D. Performance Evaluation Metrics

We measure the effectiveness of our proposed framework in terms of classification and attention performance. From the perspective of classification performance, we use accuracy (Acc), precision (P), recall (R), and F_1 score to evaluate the performance of our method comprehensively. The details of the metrics are listed as follows:

$$Acc = \frac{TP + TN}{TP + TN + FP + FN}, P = \frac{TP}{TP + FP},$$

$$R = \frac{TP}{TP + FN}, F_1 = \frac{2 \cdot P \cdot R}{P + R},$$

where TP, TN, FP, and FN are four classification results, denoting true positive, true negative, false positive, and false negative, respectively. Acc is a measure of the overall correctness of a classification model. P represents the ability of the method to distinguish anomalies, and a higher P accurately indicates fewer false anomalies. R is to determine the ability of the method to detect all the anomalies. Since the P and R metrics often appear contradictory, the F_1 score is a metric for comprehensively considering these two indicators and providing a balanced overall performance of the method. When the data set has imbalanced classes, F1 Score might be a better metric than accuracy.

In the perspective of attention accuracy performance, we adjust the relevance accuracy (RA) proposed in [23] to quantify how accurate a model is at locating ground-truth time points at which the abnormal behavior occurs. The core idea of relevance accuracy is to compare the k most attention time points for a prediction with the ground-truth abnormal time points. For a given time sequence T_i , let $G(T_i)$ denote the set of continuous or discontinuous ground-truth abnormal time points, where $|G(T_i)|$ is the number of ground-truth time points, and $R_i(k)$ denote the k time steps that get the most attention for the prediction of the model. To apply this metric to data with varying numbers of ground-truth time points, we set $k = (1 + M\%) \times |G(T_i)|$ and denote $R_i(k)$ as $R_i(M\%)$ in our work. In this analysis, the sequence of the ground-truth time points is disregarded, given that each ground-truth time point is treated with equal significance. Optimal relevance accuracy is attained when all elements of $G(T_i)$ are encompassed within $R_i(M\%)$, ideally with the minimal

possible value of M . For a time sequence T_i , $RA(T_i)$ can be calculated as:

$$RA(T_i) = \frac{|R_i(M\%) \cap G(T_i)|}{|G(T_i)|}, \quad (9)$$

where \cap is the intersection of two sets and $|\cdot|$ is the cardinality of a set. The time points the model is attention to are ranked based on CAM value before they are compared to $G(T_i)$. Therefore, simply highlighting all time points will not result in a high relevance accuracy score. The model needs to highlight some time points as being more important than others.

To assess the participants' subjective perception of human-machine cooperation, a questionnaire with a five-point Likert Scale [24] with the following items was used.

E. Datasets

Mars Science Laboratory (MSL) dataset is a dataset that corresponds to the sensor and actuator data for the Mars rover [26]. At the same time, the data set marks the time point when the abnormal behavior occurs for us to calculate relevance accuracy. However, this dataset is known to have many trivial sequences [32]; hence, to make a best-faith effort to filter out data with mislabeled ground truth time points, we build the new dataset based on the two nontrivial ones (A2 and A4), where we randomly divide the original time series into 1000 equal-length sequences, all of 800 lengths, where the ratio of labeled normal to abnormal data is 3 to 2.

The Simulation Testbed for Exploration Vehicle ECLSS (STEVE) [33] at the University of Colorado Boulder is a simplified single-bed CO_2 removal system of the Carbon Dioxide Removal Assembly (CDRA) onboard the International Space Station (ISS). A corresponding Simulink model is provided to simulate multiple failure modes similar to the STEVE testbed. In our study, we conducted a simulation consisting of four cycles, each comprising 80 minutes of CO_2 adsorption followed by 80 minutes of desorption. During the third cycle, a simulated leak failure is introduced at a random time point in *Valve 1*, resulting in observable anomalies in three sensors: *Bed Temperature*, *CO_2 Concentration*, and *Flow Rate*. These sensor sequences are treated collectively as a set of sequences. We generated 1000 sets of sequences with a ratio of 4 to 1 between labeled normal and abnormal data. Additionally, we marked the time points at which abnormal behaviors occurred in the three sensors to calculate relevance accuracy.

F. Baseline Methods

Baseline model. In this paper, we use the fully convolutional network (FCN) proposed in [34], which has demonstrated good performance on time series classification benchmarks. In addition to the baseline model, we also compare our spurious attention elimination method with the following data augmentation strategies for the same number, Q , of instances:

Random Aug. Randomly select Q instances from the training set for model fine-tuning.

Random Mask. Select the Q instances proposed by our system, but add masks at random time points for each instance.

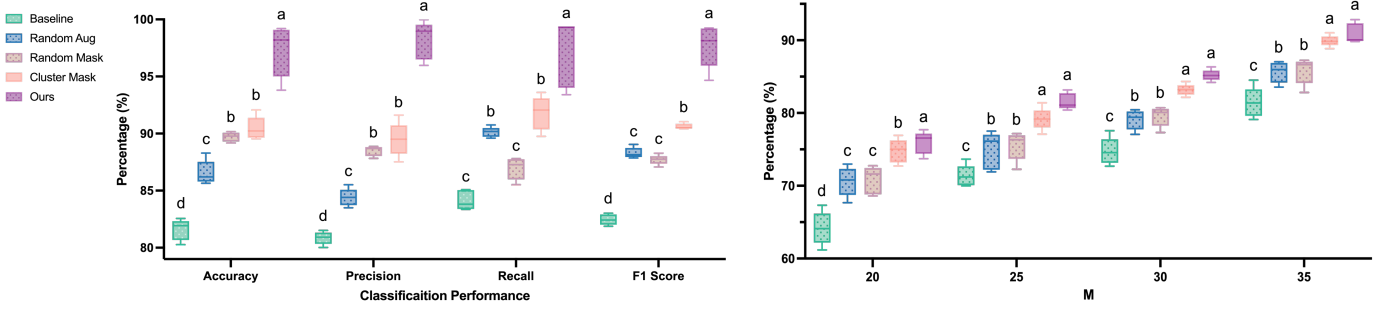


Fig. 4. Tukey HSD post-hoc test results for MSL dataset. The left plot illustrates classification performance, while the right one depicts attention accuracy. Methods not sharing any letter are significantly different by the Tukey-test at the 5% level of significance.

To further verify the effectiveness of our method, we compared the following strategy as the ablation study of our method.

Cluster Mask. The Q instances proposed by our system only concede the participant’s operation in the Cluster Information window, which means the participants in the Instance Information window make no further adjustments. This method uses the same masking strategy as ours.

G. Statistical Analysis

For Hypothesis 1, since all five methods involved in the comparison have been tested an equal number of times, we directly assess their performance using the metrics introduced in Section III-D. Therefore, our hypothesis tests reduces to:

$$\begin{aligned}
 H_0 : & \mu_{Acc1} = \dots = \mu_{Acc5}, \mu_{P1} = \dots = \mu_{P5}, \\
 & \mu_{R1} = \dots = \mu_{R5}, \mu_{F11} = \dots = \mu_{F15}, \\
 & \mu_{RA1} = \dots = \mu_{RA5}; \\
 H_1 : & \mu_{Acc1} \neq \dots \neq \mu_{Acc5}, \mu_{P1} \neq \dots \neq \mu_{P5}, \\
 & \mu_{R1} \neq \dots \neq \mu_{R5}, \mu_{F11} \neq \dots \neq \mu_{F15}, \\
 & \mu_{RA1} \neq \dots \neq \mu_{RA5}.
 \end{aligned}$$

To evaluate participants’ subjective perceptions of human-AI cooperation, we administered a questionnaire featuring a five-point Likert scale designed to assess key aspects such as intuition, transparency, and reliability. In this subjective evaluation, we compare three methods: (1) Random Augmentation, driven by a purely automatic algorithm. When employing this method, only the System Menu is accessible within our interactive interface, and the user interaction is limited to operating the retrain button; (2) Human-AI Cluster Mask, which, upon execution, presents windows A, B, and C on our interface. Users can assess the correctness of attention by clusters but lack the capability to inspect and adjust individual data points within each cluster; (3) Human-AI *HILAD*, the comprehensive version, where users are allowed to refine their assessments in window D. By contrasting (1) with (2) and (3), we aim to elucidate the impact of increasing user engagement on subjective evaluation. Conversely, by contrasting (2) with (3), we seek to discern the added benefits by enabling detailed individual data adjustments within the clusters.

IV. RESULTS

In order to effectively measure the objective performance difference between purely automatic algorithm-driven and

human-machine cooperative anomaly detection methods, we conducted an analysis using Analysis of Variance (ANOVA) tests [35]. Objective performance is divided into two aspects, namely classification correctness and attention correctness. For the former, we utilize the ANOVA test to compare the means of accuracy, precision, recall, and F1 score across different models to statistically ascertain any significant performance variations. For the latter, we employed the ANOVA test to determine whether there are statistically significant differences in relevance accuracy at varying levels of M , specifically at $M = 20, 25, 30$, and 35 . Upon identifying significant differences with the ANOVA test, we proceeded with the Tukey HSD post-hoc test to further distinguish which specific group means, among the compared groups, are significantly different from each other, ensuring a thorough evaluation of pairwise contrasts. Owing to space limitations, this article presents only the results of the Tukey HSD post-hoc test for two datasets, as illustrated in Fig. 4 and Fig. 5, respectively.

The result of the five-point Likert scale for objective evaluation is shown in Fig. 6. For a more comprehensive analysis, we also furnish the post-test results for the three methods, assessing their comparative effectiveness using a t-test. The stars intended to flag levels of significance as shown in Fig. 6 are based on the adjusted p-values.

V. DISCUSSION

A. Hypothesis 1

Firstly, regarding classification correctness, Fig. 4 demonstrates that on univariate data, all data augmentation methods significantly enhance the model’s classification performance compared to the baseline model. Among these methods, within the context of human-AI cooperation, the **Cluster Mask** approach does not exhibit a significant difference from the **Random Mask** in the automatic method across other metrics, with the exception of the F1 score. However, our method demonstrated significant enhancements in all four metrics of classification performance when compared to all other methods. Compared to approach **Cluster Mask**, the improvement in our approach is facilitated by the **D** window’s functionality, which enables humans to further refine the automatic clustering algorithm. This aspect also contributes to the observed large variance in our method across the four metrics, reflecting the variability in human judgment and adjustments.

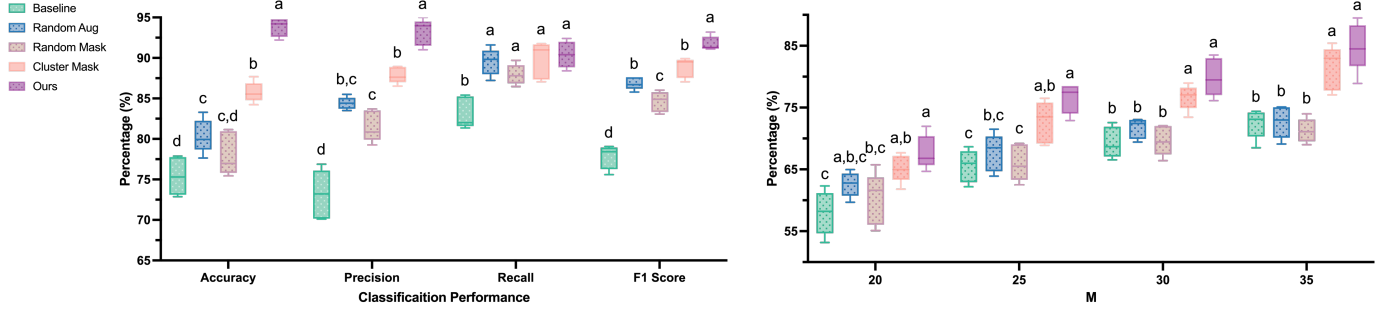


Fig. 5. Tukey HSD post-hoc test results for STEVE dataset. The left plot illustrates classification performance, while the right one depicts attention accuracy. Methods not sharing any letter are significantly different by the Tukey-test at the 5% level of significance.

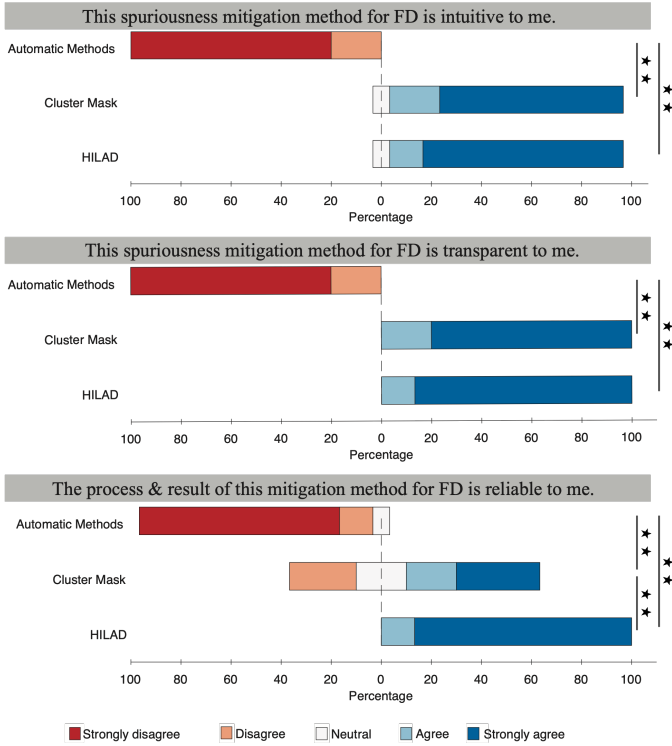


Fig. 6. Participants' perception of the system, according to nine Likert-Type Questions using a 5-point scale.

This variability is partly due to the high number of instances in each cluster. Despite this, in terms of overall performance, the adjustments made by humans do yield beneficial outcomes.

As depicted in Fig. 5, similar to the univariate data, all data augmentation methods, with the exception of the accuracy metric for the **Random Mask** approach, show results that are significantly different from the baseline model. Furthermore, within the realm of human-AI cooperation, the **Cluster Mask** approach exhibits a significant difference over other automatic algorithms solely in terms of accuracy. However, our method demonstrates significant differences from both other automatic data augmentation methods and the **Cluster Mask** method in terms of accuracy, precision, and F1 score. In terms of recall, no significant differences are observed among all data augmentation methods. This phenomenon can be attributed to the imbalanced nature of the dataset, where the abundance

of normal instances prompts the model to occasionally misclassify abnormal instances as normal. In such imbalanced datasets, neither recall nor precision in isolation serves as a reliable measure of method performance. Instead, the F1 score emerges as a more accurate metric due to its ability to strike a balance between precision and recall.

Shifting our focus to attention accuracy, both the cluster mask and our method exhibit significant deviations from other automatic algorithms when applied to univariate data. However, as the data dimensionality increases, achieving accurate attention becomes increasingly challenging, particularly at $M = 20$, where no significant disparities exist between the cluster mask method and other automatic algorithms. Nevertheless, consistent disparities persist between our methods and the automatic algorithm. A more in-depth analysis reveals that, despite the notable improvements in classification performance when compared to the baseline model, the automatic algorithm fails to significantly enhance attention accuracy, especially concerning multivariate data. This observation reinforces the notion that our method not only objectively enhances classification performance but also elevates attention accuracy, thereby bolstering overall system reliability.

In summary, our method exhibits substantial deviations in both classification correctness and attention correctness when compared to the automatic algorithm across the two datasets. This substantiates our conjecture and underscores the empirical evidence supporting our approach.

B. Hypothesis 2

In the subjective evaluation, both the cluster mask method and our method are significantly different from the automatic algorithm in intuition, transparency, and reliability. Because the automatic algorithm can only provide the result of classification, it cannot provide the criterion of classification. The cluster mask method is not significantly different from intuition and transparency, as both provide reasons for the model to make a prediction. But on reliability, we are significantly different from the cluster mask method because of the error of the automatic clustering algorithm itself, while in our method, the **D** window can provide more detailed options to further correct the automatic algorithm, which helps improve performance objectively. At the same time, humans are subjectively more likely to believe that our methods are more reliable.

Therefore, we verified that subjectively human-AI method has significant improvement in intuition, transparency, and reliability compared with automatic algorithms, thus verifying Hypothesis 2. Further, on the objective and subjective level, the necessity of introducing **D** window is verified by comparing with **Cluster Mask** method.

VI. CONCLUSION

In conclusion, we introduce a human-AI collaboration framework, *HILAD*, to enhance the performance and reliability of time series anomaly detection models. With our interactive visual interface, human expertise can be effectively leveraged to detect and eliminate the hidden model biases in scale. Through objective and subjective evaluations with two benchmark datasets, we demonstrate the exceptional capabilities of *HILAD* in enhancing the model's classification accuracy and attention correctness. With *HILAD*, we underscore the potential of human-AI collaboration in supporting greater transparency, reliability, and trustworthiness of machine learning models. We hope the design of how human expertise can be effectively leveraged in our work can inspire the development of next-generation trustworthy AI systems.

REFERENCES

- [1] M. Ahmed, A. N. Mahmood, and M. R. Islam, "A survey of anomaly detection techniques in financial domain," *Future Generation Computer Systems*, vol. 55, pp. 278–288, 2016.
- [2] E. Šabić, D. Keeley, B. Henderson, and S. Nannemann, "Healthcare and anomaly detection: using machine learning to predict anomalies in heart rate data," *AI & SOCIETY*, vol. 36, no. 1, pp. 149–158, 2021.
- [3] D. Li, D. Chen, B. Jin, L. Shi, J. Goh, and S.-K. Ng, "Mad-gan: Multivariate anomaly detection for time series data with generative adversarial networks," in *International conference on artificial neural networks*. Springer, 2019, pp. 703–716.
- [4] T. Kieu, B. Yang, C. Guo, and C. S. Jensen, "Outlier detection for time series with recurrent autoencoder ensembles," in *IJCAI*, 2019, pp. 2725–2732.
- [5] P. Malhotra, L. Vig, G. Shroff, P. Agarwal *et al.*, "Long short term memory networks for anomaly detection in time series," in *Esann*, vol. 2015, 2015, p. 89.
- [6] S. J. Taylor and B. Letham, "Forecasting at scale," *The American Statistician*, vol. 72, no. 1, pp. 37–45, 2018.
- [7] F. A. Del Campo, M. C. G. Neri, O. O. V. Villegas, V. G. C. Sánchez, H. d. J. O. Domínguez, and V. G. Jiménez, "Auto-adaptive multilayer perceptron for univariate time series classification," *Expert Systems with Applications*, vol. 181, p. 115147, 2021.
- [8] C. Gallicchio, A. Micheli, L. Silvestri *et al.*, "Local Lyapunov exponents of deep rnn," in *Proceedings of the 25th European Symposium on Artificial Neural Networks (ESANN)*. i6doc. com publication, 2017, pp. 559–564.
- [9] B. Zhao, H. Lu, S. Chen, J. Liu, and D. Wu, "Convolutional neural networks for time series classification," *Journal of Systems Engineering and Electronics*, vol. 28, no. 1, pp. 162–169, 2017.
- [10] E. Nabrawi and A. Alanazi, "Fraud detection in healthcare insurance claims using machine learning," *Risks*, vol. 11, no. 9, p. 160, 2023.
- [11] T. Meena and S. Roy, "Bone fracture detection using deep supervised learning from radiological images: A paradigm shift," *Diagnostics*, vol. 12, no. 10, p. 2420, 2022.
- [12] S. Uddin, A. Khan, M. E. Hossain, and M. A. Moni, "Comparing different supervised machine learning algorithms for disease prediction," *BMC medical informatics and decision making*, vol. 19, no. 1, pp. 1–16, 2019.
- [13] M. T. Ribeiro, S. Singh, and C. Guestrin, "“why should I trust you?”: Explaining the predictions of any classifier," in *Proceedings of the 22nd ACM SIGKDD International Conference on Knowledge Discovery and Data Mining, San Francisco, CA, USA, August 13-17, 2016*, 2016, pp. 1135–1144.
- [14] S. M. Lundberg and S.-I. Lee, "A unified approach to interpreting model predictions," in *Advances in Neural Information Processing Systems 30*, I. Guyon, U. V. Luxburg, S. Bengio, H. Wallach, R. Fergus, S. Vishwanathan, and R. Garnett, Eds. Curran Associates, Inc., 2017, pp. 4765–4774. [Online]. Available: <http://papers.nips.cc/paper/7062-a-unified-approach-to-interpreting-model-predictions.pdf>
- [15] Y. Zhang, K. Song, Y. Sun, S. Tan, and M. Udell, "“ why should you trust my explanation?” understanding uncertainty in lime explanations," *arXiv preprint arXiv:1904.12991*, 2019.
- [16] J. Dieber and S. Kirrane, "Why model why? assessing the strengths and limitations of lime," *arXiv preprint arXiv:2012.00093*, 2020.
- [17] H. T. T. Nguyen, H. Q. Cao, K. V. T. Nguyen, and N. D. K. Pham, "Evaluation of explainable artificial intelligence: Shap, lime, and cam," in *Proceedings of the FPT AI Conference*, 2021, pp. 1–6.
- [18] S. Weinzierl, S. Zilker, J. Brunk, K. Revoreda, M. Matzner, and J. Becker, "Xnap: making lstm-based next activity predictions explainable by using lrp," in *International Conference on Business Process Management*. Springer, 2020, pp. 129–141.
- [19] B. Lim, S. Ö. Arık, N. Loeff, and T. Pfister, "Temporal fusion transformers for interpretable multi-horizon time series forecasting," *International Journal of Forecasting*, vol. 37, no. 4, pp. 1748–1764, 2021.
- [20] L. Schwenke and M. Atzmueller, "Abstracting local transformer attention for enhancing interpretability on time series data," in *LWDA*, 2021, pp. 205–218.
- [21] B. Zhou, A. Khosla, A. Lapedriza, A. Oliva, and A. Torralba, "Learning deep features for discriminative localization," in *Proceedings of the IEEE conference on computer vision and pattern recognition*, 2016, pp. 2921–2929.
- [22] R. R. Selvaraju, M. Cogswell, A. Das, R. Vedantam, D. Parikh, and D. Batra, "Grad-cam: Visual explanations from deep networks via gradient-based localization," in *Proceedings of the IEEE international conference on computer vision*, 2017, pp. 618–626.
- [23] K. Wickstrøm, K. Ø. Mikalsen, M. Kampffmeyer, A. Revhaug, and R. Jenssen, "Uncertainty-aware deep ensembles for reliable and explainable predictions of clinical time series," *IEEE Journal of Biomedical and Health Informatics*, vol. 25, no. 7, pp. 2435–2444, 2020.
- [24] D. Jung, N. Ramanan, M. Amjadi, S. R. Karingula, J. Taylor, and C. N. Coelho Jr, "Time series anomaly detection with label-free model selection," *arXiv preprint arXiv:2106.07473*, 2021.
- [25] M. Goswami, C. Challu, L. Callot, L. Minorics, and A. Kan, "Unsupervised model selection for time-series anomaly detection," *arXiv preprint arXiv:2210.01078*, 2022.
- [26] K. Hundman, V. Constantinou, C. Laporte, I. Colwell, and T. Soderstrom, "Detecting spacecraft anomalies using lstms and nonparametric dynamic thresholding," in *Proceedings of the 24th ACM SIGKDD international conference on knowledge discovery & data mining*, 2018, pp. 387–395.
- [27] L. McInnes, J. Healy, and J. Melville, "Umap: Uniform manifold approximation and projection for dimension reduction," *arXiv preprint arXiv:1802.03426*, 2018.
- [28] K. Krishna and M. N. Murty, "Genetic k-means algorithm," *IEEE Transactions on Systems, Man, and Cybernetics, Part B (Cybernetics)*, vol. 29, no. 3, pp. 433–439, 1999.
- [29] D. Zhou, O. Bousquet, T. Lal, J. Weston, and B. Schölkopf, "Learning with local and global consistency," *Advances in neural information processing systems*, vol. 16, 2003.
- [30] S. Singla, M. Moayeri, and S. Feizi, "Core risk minimization using salient imagenet," *arXiv preprint arXiv:2203.15566*, 2022.
- [31] P. Tang and X. Zhang, "Mtsmae: Masked autoencoders for multivariate time-series forecasting," in *2022 IEEE 34th International Conference on Tools with Artificial Intelligence (ICTAI)*. IEEE, 2022, pp. 982–989.
- [32] R. Wu and E. J. Keogh, "Current time series anomaly detection benchmarks are flawed and are creating the illusion of progress," *IEEE transactions on knowledge and data engineering*, vol. 35, no. 3, pp. 2421–2429, 2021.
- [33] Z. Deng, S. P. Eshima, J. Nabity, and Z. Kong, "Causal signal temporal logic for the environmental control and life support system's fault analysis and explanation," *IEEE Access*, vol. 11, pp. 26471–26482, 2023.
- [34] Z. Wang, W. Yan, and T. Oates, "Time series classification from scratch with deep neural networks: A strong baseline," in *2017 International joint conference on neural networks (IJCNN)*. IEEE, 2017, pp. 1578–1585.
- [35] L. St. S. Wold *et al.*, "Analysis of variance (anova)," *Chemometrics and intelligent laboratory systems*, vol. 6, no. 4, pp. 259–272, 1989.